

Supporting Information

PyA-cluster system for detection and imaging of miRNA in living cells through double-three-way junction formation

Jong Jin Ro, Ha Jung Lee and Byeang Hyeon Kim*

Department of Chemistry, Division of Advanced Materials Science, Pohang University of Science and Technology (POSTECH), Pohang 37673, Republic of Korea

Contents

Page

- S4–6** Experimental details
- S7** **Table S1.** ^{Py}A-Modified oligonucleotide sequences of probes for the target miR-21.
Table S2. ^{Py}A-Modified oligonucleotide sequences of probes for various target miRNAs.
- S8** **Figure S1.** Normalized fluorescence emission spectra of probes in the absence (and presence) of miR-21.
- S9** **Figure S2.** Fluorescence intensity ratios of probes at 455 and 600 nm and changes to I_{455}/I_{600} in the absence and presence of miRNA.
- S10** **Table S3.** Fluorescence emission peak areas of ^{Py}A-modified probes in the presence and absence of miR-21.
- S11** **Figure S3.** Photographs of solution of ^{Py}A-modified **TWN** in the absence and presence of miR-21.
- S12** **Figure S4.** Fluorescence emission spectra and normalized fluorescence emission spectra of **TW7** in the presence of different concentrations of miR-21 from 0 to 200 nM
Figure S5. Fluorescence emission spectra and normalized fluorescence emission spectra of the **TW7-T** series.
- S13** **Figure S6** Normalized fluorescence emission spectra and fluorescence emission peak areas of ^{Py}A-modified probes in the presence and absence of miR-21.
- S14** **Figure S7.** Native PAGE images of **TW7**, **TW7-2T**, **TW7-3T**, and **TW7-4T** in the presence and absence of miR-21.
- S15** **Figure S8.** Native PAGE images of **TW7** recorded in the presence of various amounts of miR-21.
- S16** **Figure S9.** Native PAGE images of **TW7-M1** and **TW7-M2** recorded in the presence of miR-21 and miR-192.
- S17** **Figure S10.** Fluorescence emission spectra and normalized fluorescence emission spectra of probes in the presence of RNAs.
- S18** **Figure S11.** Normalized fluorescence spectra of probes in the presence and absence of miR-13, miR-192 and miR-221.
- S19** **Figure S12.** Fluorescence emission spectra, fluorescence intensity ratios compared at 455 and 600 nm, and changes in the values of I_{455}/I_{600} in the absence and presence of miRNA.

Table S4. Fluorescence emission peak areas of ^PVA-modified probes in the presence and absence of miRNAs.

- S20** **Figure S13.** Confocal microscopy images of intracellular miR-21 in living HeLa cells, recorded in the presence of **TW7**.
- S21** **Figure S14.** Confocal microscopy images of intracellular miR-21 in living HeLa cells, recorded in the absence of **TW7**.
- S22** **Figure S15.** Confocal microscopy images of intracellular miR-21 in living HeLa cells, recorded in the presence of **TW7-R**.
- S23** **Figure S16.** Confocal microscopy images of intracellular miR-21 target in living MCF-7 cells, recorded in the presence of **TW7**.
- S24** **Figure S17.** Confocal microscopy images of intracellular miR-21 target in living MCF-7 cells, recorded in the absence of **TW7**.
- S25** **Figure S18.** Confocal microscopy images of intracellular miR-21 target in living MCF-7 cells, recorded in the presence of **TW7-R**.
- S26** **Figure S19.** Confocal microscopy images of intracellular miR-21 target in living NIH-3T3 cells, recorded in the presence of **TW7**.
- S27** **Figure S20.** Confocal microscopy images of intracellular miR-21 target in living NIH-3T3 cells, recorded in the absence of **TW7**.
- S28** **Figure S21.** Confocal microscopy images of intracellular miR-21 target in living NIH-3T3 cells, recorded in the presence of **TW7-R**.
- S29** **Figure S22.** z-Stack slice images of HeLa cells, from the surface to the bottom, recorded under excitation at 405 nm.
- S30** **Figure S23.** z-Stack slice images of MCF-7 cells, from the surface to the bottom, recorded under excitation at 405 nm.
- S31** **Figure S24.** z-Stack slice images of NIH-3T3 cells, from the surface to the bottom, recorded under excitation at 405 nm.
- S32** **References**

Experimental details

Synthesis of oligonucleotides

All miRNA sequences were purchased from Integrated DNA Technologies (IDT). PyA-modified oligonucleotides (ODNs) were synthesized on a CPG support (scale: 1 μ mol; pore size: 1000 Å) using standard phosphoramidite methods and an automated DNA synthesizer (POLYGEN DNA-Synthesizer). The synthesized ODNs were cleaved from the solid support upon treatment with 28–30% aqueous NH_4OH (1.0 mL) for 12 h at 55 °C. After filtration of the CPG, the crude products from the automated ODN synthesis were lyophilized and diluted with distilled water (1 mL). The ODNs were purified through reversed-phase HPLC (Merck LichoCART C18 column; 10 \times 250 mm; 10 μ m; pore size: 100 Å). The HPLC mobile phase was held isocratically for 10 min with 5% MeCN/0.1 M triethylammonium acetate (TEAA) (pH 7.2) at a flow rate of 2.5 mL/min. The gradient was then increased linearly over 10 min from 5 to 50% MeCN/0.1 M TEAA at the same flow rate. The fractions containing the purified ODNs were cooled and lyophilized. 80% Aqueous AcOH was added to the ODNs. After 1 h at ambient temperature, the AcOH was evaporated under reduced pressure. The residue was diluted with water (1 mL); this solution was then purified through HPLC using the same conditions as those described above. The ODNs were analyzed through reversed-phase HPLC using almost the same eluent system (detection: 254 nm). The products were characterized using MALDI-TOF mass spectrometry.

ODN sample preparation

For UV spectroscopy and fluorescence spectroscopy, a solution of the ODN (1.5 μ M) was added to a solution of 50 mM Tris-HCl buffer (pH 7.2, 100 mM NaCl, 10 mM MgCl_2) and water to give a total volume of 1 mL, followed by vortex-mixing. To prepare annealed samples, the mixtures in a buffer solution were heated at 90 °C for 3 min, then slowly cooled under ambient conditions for 4 h.

UV and fluorescence spectra

UV and fluorescence spectra were recorded using Cary 100 and Eclipse spectrometers (Varian), respectively, and are reported as an average of three independent measurements. Samples for UV and fluorescence spectroscopy were prepared in a quartz cell (path length: 1 cm). For the UV spectra, all samples were measured after baseline correction. Parameters for fluorescence spectra : excitation wavelength, 380 nm; scanning range, 390–750 nm; excitation and emission slits, 2.5 nm/5 nm; data interval, 1.0 nm.

10% Native polyacrylamide gel electrophoresis (PAGE)

40% Acrylamide (2.5 mL), 5X TBE buffer (2 mL), and distilled water (5.5 mL) were mixed to obtain a 10% non-denaturing gel. Ammonium persulfate (12 mg) was added to the mixed solution. For initiation of gel formation, *N, N, N, N*-tetramethylethylenediamine (TEMED, 10 μ L) was added. Aliquot (200 pmol) of the samples were used for PAGE. The dried samples were dissolved in buffer/formamide mixture (10 μ L; 1:1, v/v) for sample loading. Conditions for PAGE : 90 V; 34 mA; 3 W; 25 $^{\circ}$ C; 2 h. After running, the gels were mixed with Stains-all (Sigma- Aldrich) in formamide for 30 min. Gels were dried and exposed to light for visualization of the DNA bands.

Gel permeation chromatography (GPC)

GPC was performed using a Shimadzu GPC system, equipped with two consecutive Styragel columns (Shodex-OHpak SB-806M and SB-803) and a Shimadzu RID-10A refractive index detector. Water was used as the eluent at a flow rate of 1 mL/min. A series of PEG standards were used for calibration.¹

Preparation of cell samples and their confocal microscopy imaging

Three cell lines (HeLa, MCF-7, NIH-3T3) were provided by Professor C. Ban (Pohang university of science and technology, Pohang, Republic of Korea). The cell lines were incubated in Dulbecco modified Eagle Medium (DMEM) or Roswell Park Memorial Institute medium (RPMI) supplemented with 10% (v/v) fetal bovine serum (FBS) and 1% (v/v) penicillin / streptomycin (PS) at 37°C in a humidified atmosphere of 5% of CO₂ in air. After the cells has been cultured on a circular dish, they were trypsinized and resuspended in DMEM (or RPMI) media. Aliquots (3 μL) containing 3×10^3 cells were sub-cultured to 80% (v/v) occupation on a circular dish in the humid CO₂ incubator.² For imaging experiments, the cells were incubated in DMEM (or RPMI) containing the probe **TW7** (0.4 μM) and Lipofectamine 3000 transfection reagent (*ThermoFisher Scientific*) for 24 - 36 h and then washed with phosphate-buffered saline (PBS) to remove any remaining probe. In the control experiment with **TW7-R** (featuring a random sequence at the binding site for the miRNA), the cells were co-incubated in DMEM (or RPMI) containing the probe at the same concentration. The medium was replaced with Gibco Opti-MEM (*ThermoFisher Scientific*) after washing the cells with PBS to remove any traces of the residual medium. Fluorescence images of the cell samples were recorded using confocal microscopy. Confocal imaging was performed using an all-channels spectral confocal laser scanning microscope for multi-photon imaging (TCS SP5 II, Leica, Germany). The confocal excitation wavelength for the probe was tuned to 405 nm. Each emission was spectrally resolved into two channels ($\lambda_{em,blue} = 455\text{--}495$ nm; $\lambda_{em,yellow} = 555\text{--}600$ nm). The images comprised 1024×1024 pixels; the scanning speed was maintained at 200 MHz throughout the imaging process. Acquired images were processed using LAS AF Lite software (Leica, Germany); all the images were converted into corresponding pixel-to-pixel ratiometric images based on the intensity ratio of I_{Blue}/I_{Yellow} .³

Table S1. ^{Py}A-Modified oligonucleotide sequences of probes for the target miR-21.**Target RNA sequences****miR-21** (22-mer): 5'-uag cuu auc aga cug aug uug a-3'**^{Py}A-modified oligonucleotide probe sequences**

Name	Sequence (5' → 3')	Calculated MS (<i>m/z</i>)	Observed MS (<i>m/z</i>)
TW1	TCA ACA TCA GT AA ^{Py} AAA AA ^{Py} AAA C TGA TAA GCT A	10278.5593	10278.6421
TW2	TCA ACA TCA GT AA ^{Py} AAA C AA ^{Py} AAA C TGA TAA GCT A	10567.6062	10567.8746
TW3	TCA ACA TCA GT AA ^{Py} AAA CG AA ^{Py} AAA C TGA TAA GCT A	10896.6593	10896.4315
TW4	TCA ACA TCA GT AA ^{Py} AAA CGC AA ^{Py} AAA C TGA TAA GCT A	11185.7062	11185.7851
TW5	TCA ACA TCA GT AA ^{Py} AAA CGCG AA ^{Py} AAA C TGA TAA GCT A	11514.7593	11514.1239
TW6	TCA ACA TCA GT AA ^{Py} AAA CGCGC AA ^{Py} AAA C TGA TAA GCT A	11803.8062	11803.7432
TW7	TCA ACA TCA GT AA ^{Py} AAA (CG) ₃ AA ^{Py} AAA C TGA TAA GCT A	12132.8593	12132.6654
TW8	TCA ACA TCA GT AA ^{Py} AAA (CG) ₄ AA ^{Py} AAA C TGA TAA GCT A	12750.9593	12750.7546
TW9	TCA ACA TCA GT AA ^{Py} AAA (CG) ₅ AA ^{Py} AAA C TGA TAA GCT A	13369.0593	13369.1284
TW10	TCA ACA TCA GT AA ^{Py} AAA (CG) ₆ AA ^{Py} AAA C TGA TAA GCT A	13987.1593	13987.2131
TW7-2T	TCA ACA TCA GT AA ^{Py} AAA CGC TT GCG AA ^{Py} AAA C TGA TAA GCT A	12740.2813	12739.2813
TW7-3T	TCA ACA TCA GT AA ^{Py} AAA CGC TTT GCG AA ^{Py} AAA C TGA TAA GCT A	13044.3279	13043.4876
TW7-4T	TCA ACA TCA GT AA ^{Py} AAA CGC TTTT GCG AA ^{Py} AAA C TGA TAA GCT A	13348.3745	13347.9279

Table S2. ^{Py}A-Modified oligonucleotide sequences of probes for various target miRNAs.**Target RNA sequences****miR-13** (22-mer): 5'-uau cac agc cau uuu gau gag u-3'**miR-192** (21-mer): 5'-cug acc uau gaa uug aca gcc-3'**miR-221** (21-mer): 5'-auu ucu gug uuc guu agg caa-3'

Name	Sequence (5' → 3')	Calculated MS (<i>m/z</i>)	Observed MS (<i>m/z</i>)
TW-m13	ACT CAT CAA AA AA ^{Py} AAA (CG) ₃ AA ^{Py} AAA TGG CTG TGA TA	12172.8655	12172.6541
TW-m192	GGC TGT CAA TT AA ^{Py} AAA (CG) ₃ AA ^{Py} AAA CAT AGG TCA G	11891.7974	11891.6475
TW-m221	TTG CCT AAC AA ^{Py} AAA (CG) ₃ AA ^{Py} AAA GAA CAC AGA AAT	11837.8242	11837.7564

Figure S1. Normalized fluorescence emission spectra of probes in the absence and presence of miR-21. (A) **TW1**, (B) **TW2**, (C) **TW3**, (D) **TW4**, (E) **TW5**, (F) **TW6**, (G) **TW7**, (H) **TW8**, (I) **TW9**, (J) **TW10**, and (K) summary

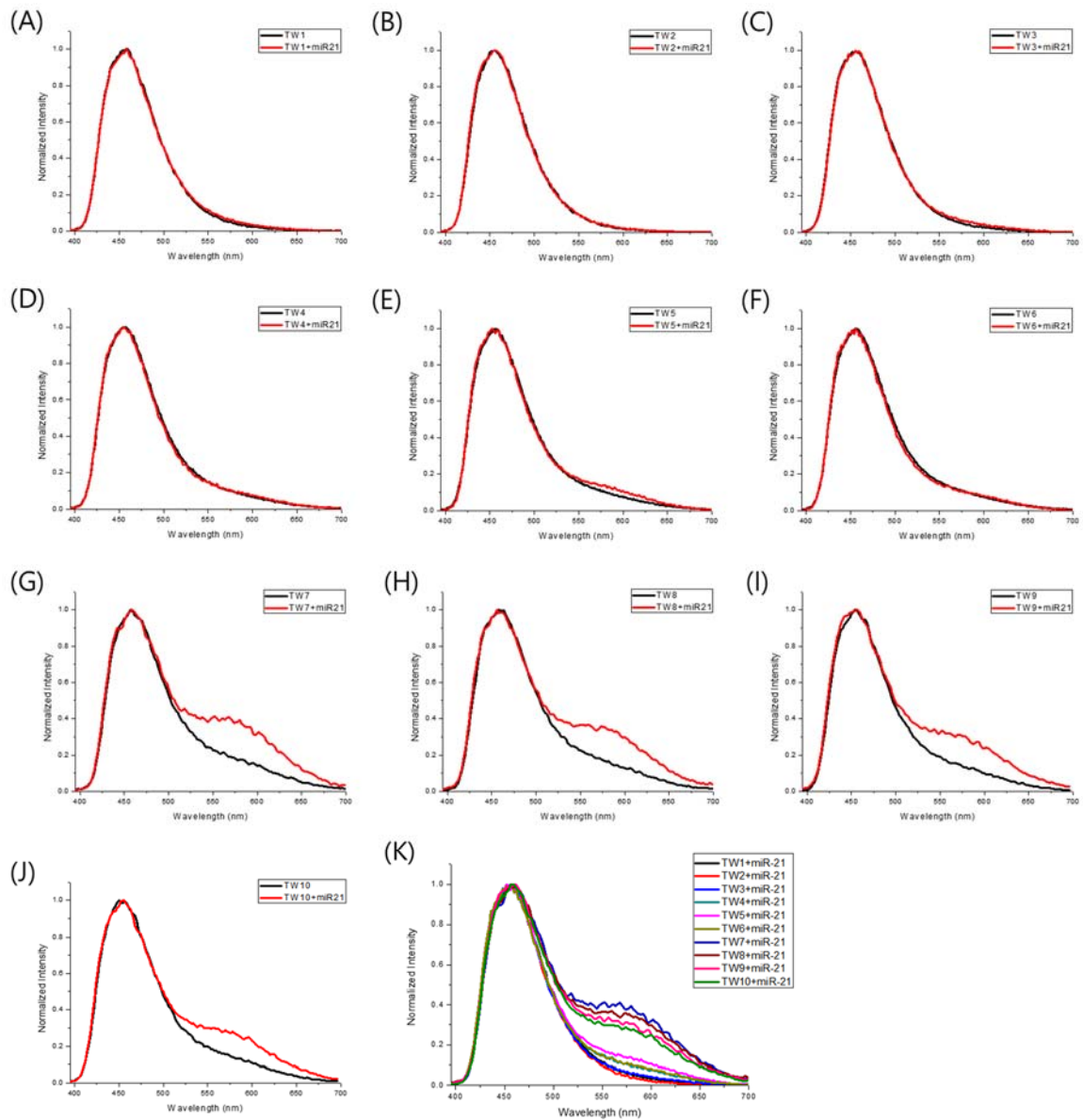
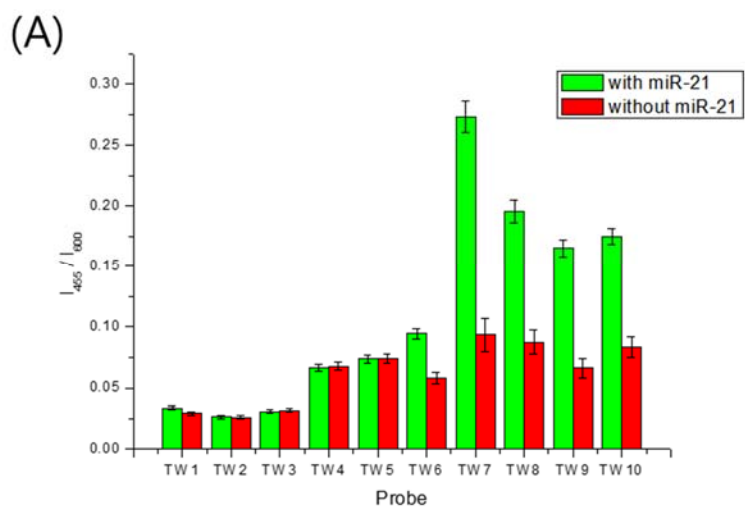


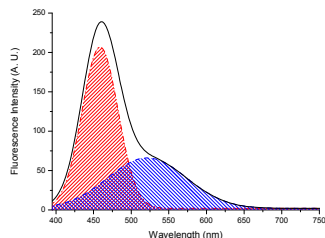
Figure S2. (A) Fluorescence intensity ratios of probes at 455 and 600 nm and (B) changes to I_{455}/I_{600} in the absence and presence of miRNA.



(B)

Probe	$F - F_0$
TW1	0.004
TW2	0.000
TW3	-0.001
TW4	-0.001
TW5	0.000
TW6	0.037
TW7	0.180
TW8	0.108
TW9	0.099
TW10	0.091

Table S3. Fluorescence emission peak areas of PyA-modified probes in the presence and absence of miR-21.



ODNs	1 st area ^a	1 st area%	2 nd area ^b	2 nd area%	$A_{\text{long}}/A_{\text{short}}$
TW7+miR21	6148	43	8389	57	1.3645
TW8+miR-21	7467	46	8787	54	1.1768
TW9+miR-21	9144	51	8909	49	0.9743
TW10+miR-21	8336	47	9337	53	1.1200

ODNs	1 st area ^a	1 st area%	2 nd area ^b	2 nd area%	$A_{\text{long}}/A_{\text{short}}$
TW7	12285	59	8398	41	0.6836
TW8	11835	60	7975	40	0.6738
TW9	12498	57	9153	43	0.7324
TW10	12630	60	8491	40	0.6723

^a Area percentage of the fluorescence emission peak at 455 nm. ^b Area percentage of the fluorescence emission peak at 575 nm. All spectra were recorded for samples in buffer (50 mM Tris-HCl, 100 mM NaCl, 10 mM MgCl₂; pH 7.2) at 25 °C.

Figure S3. Photographs of solutions of ^{PyA}-modified **TWN** in the absence and presence of miR-21.

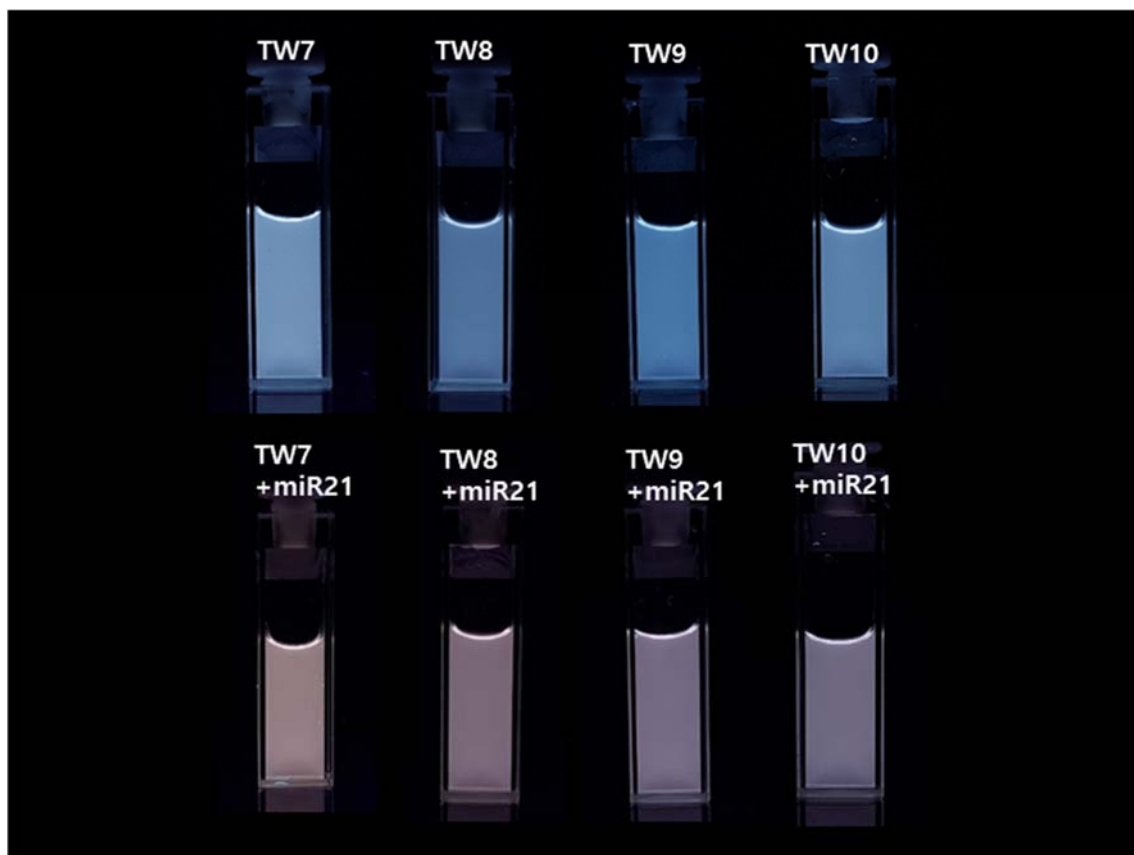


Figure S4. (A) Fluorescence emission spectra and (B) normalized fluorescence emission spectra of **TW7** (100 nM) in the presence of different concentrations of miR-21 from 0 to 200 nM. (C) The linear relation ($R^2 = 0.9861$) between the fluorescence change and the concentration of miR-21. Parameters for fluorescence spectra : excitation wavelength, 380 nm; scanning range, 390–700 nm; excitation and emission slits, 5 nm/5 nm; data interval, 1.0 nm.

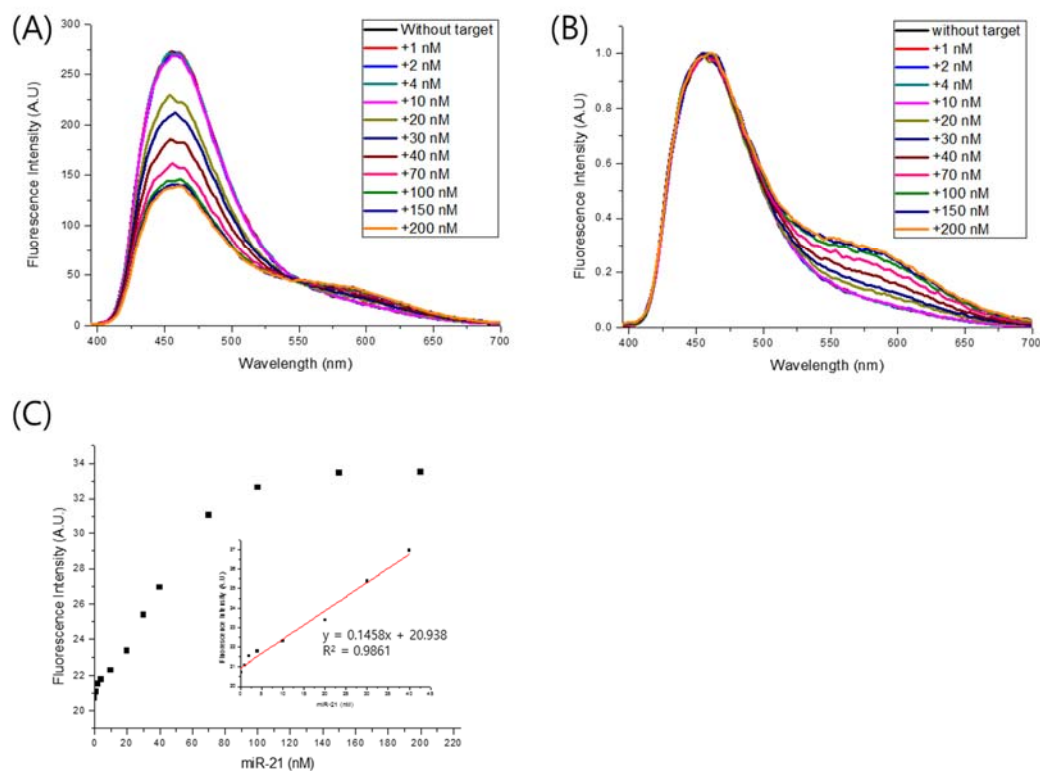


Figure S5. (A) Fluorescence emission spectra and (B) normalized fluorescence emission spectra of the **TW7-T** series.

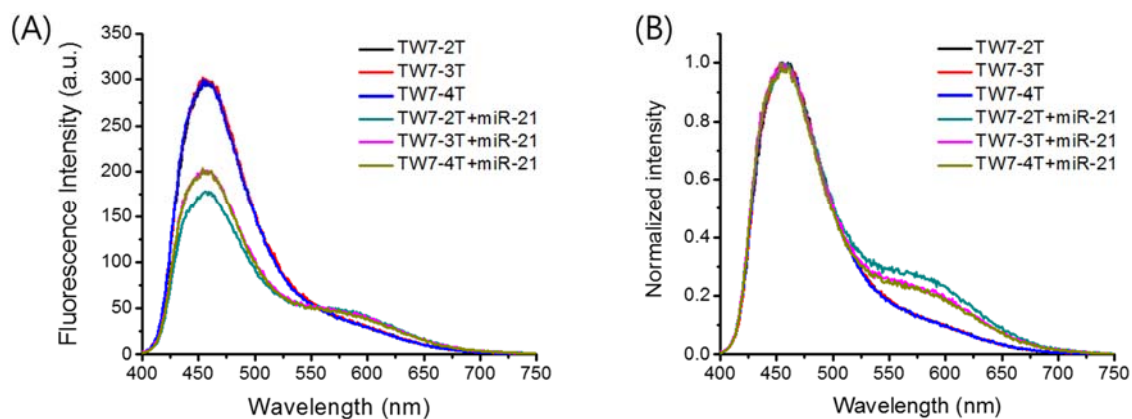
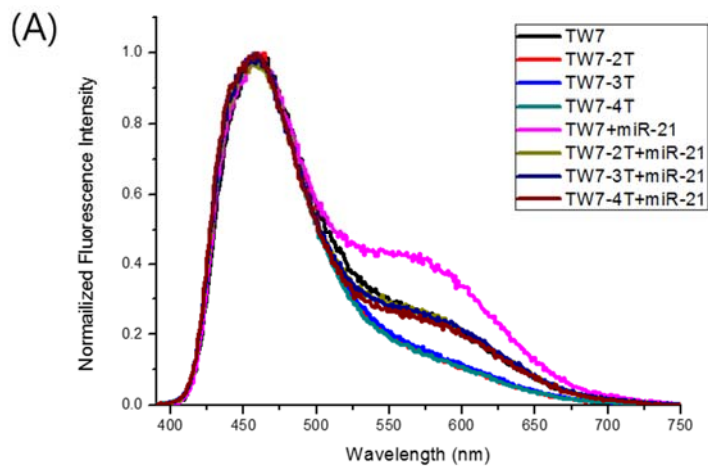


Figure S6. (A) Normalized fluorescence emission spectra and (B) fluorescence emission peak areas of ^{Py}A-modified probes in the presence and absence of miR-21.



(B)	ODNs	1 st area ^a	1 st area %	2 nd area ^b	2 nd area %	$A_{\text{long}} / A_{\text{short}}$
	TW7+miR-21	6148	43	8389	57	1.3645
	TW7-2T+miR-21	9530	50	9556	50	1.0027
	TW7-3T+miR-21	10371	50	10260	50	0.9893
	TW7-4T+miR-21	9369	52	8730	48	0.9318
	TW7	12285	59	8398	41	0.6836
	TW7-2T	13998	59	9601	41	0.6859
	TW7-3T	14646	59	10107	41	0.6901
	TW7-4T	12775	60	8564	40	0.6704

^a Area percentage of the fluorescence emission peak at 455 nm. ^b Area percentage of the fluorescence emission peak at 575 nm. All spectra were recorded for samples in buffer (50 mM Tris-HCl, 100 mM NaCl, 10 mM MgCl₂; pH 7.2) at 25 °C.

Figure S7. Native PAGE images of **TW7**, **TW7-2T**, **TW7-3T**, and **TW7-4T** in the presence and absence of miR-21, (A) stained with Stains-All and (B) under UV irradiation.

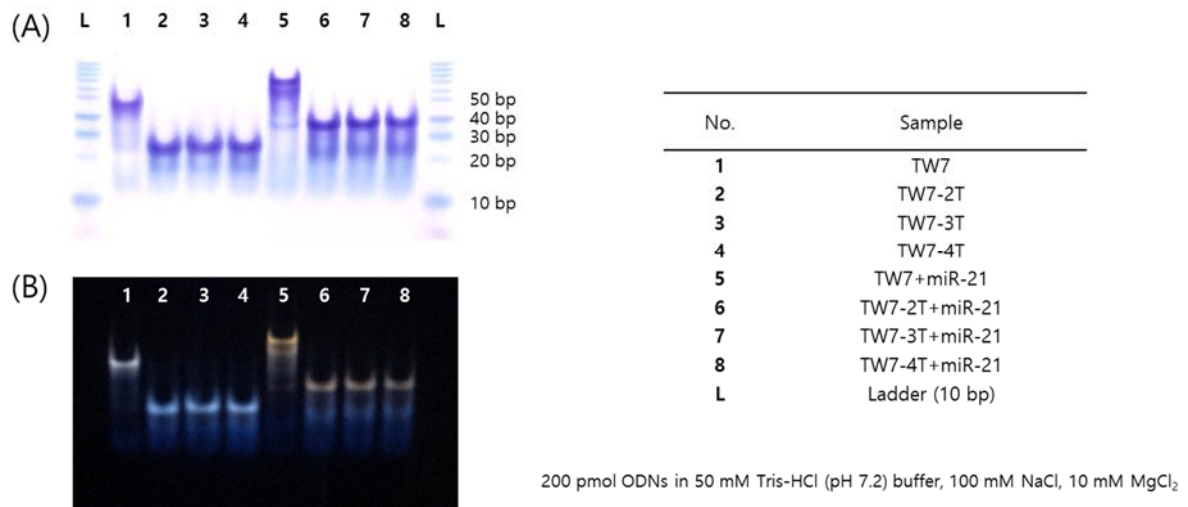


Figure S8. Native PAGE images of **TW7** recorded in the presence of various amounts of miR-21, (A) stained with Stains-All and (B) under UV irradiation.

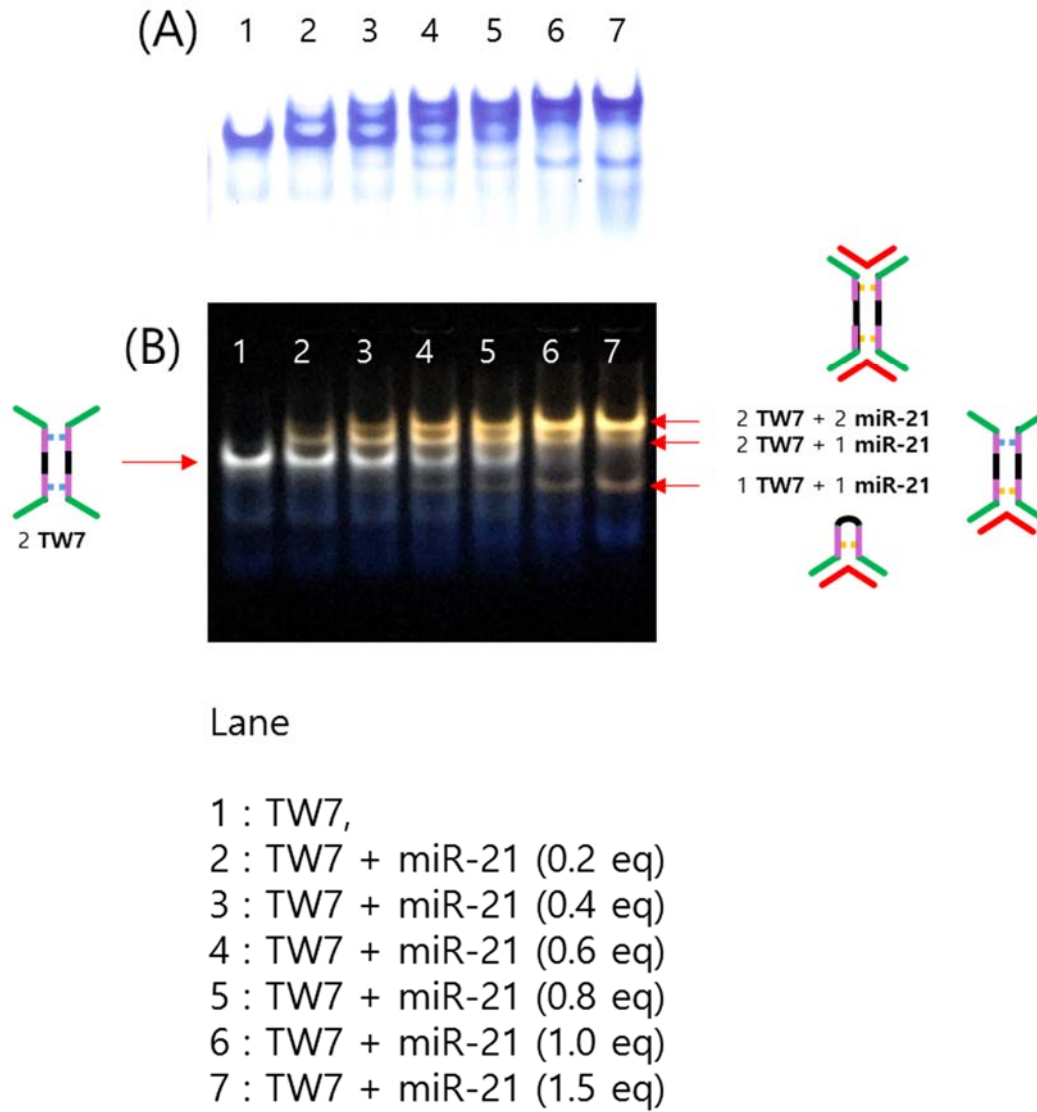
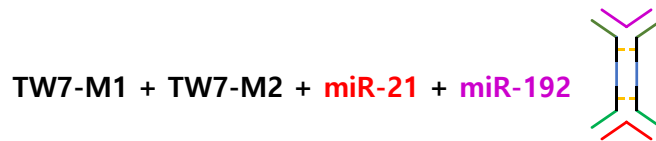


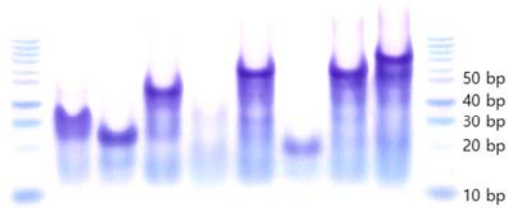
Figure S9. Native PAGE images of **TW7-M1** and **TW7-M2** recorded in the presence of miR-21 and miR-192, (A) stained with Stains-All and (B) under UV irradiation.

Name	Sequence	Calculated MS (<i>m/z</i>)	Observed MS (<i>m/z</i>)
TW7	5'-TCA ACA TCA GT AA ^P AAA CGC GCG AA ^P AAA C TGA TAA GCT A-3'	12132.8593	12132.6654
TW7-M1	5'-TCA ACA TCA GT AA ^P AAA CGG CGG AA ^P AAA CAT AGG TCA G-3'	11884.1427	11885.6643
TW7-M2	5'-GGC TGT CAA TT AA ^P AAA CCG CCG AA ^P AAA C TGA TAA GCT A-3'	12139.1716	14140.1834
miR-21	5'-uag cuu auc aga cug aug uug a-3'		
miR-192	5'-cug acc uau gaa uug aca gcc-3'		

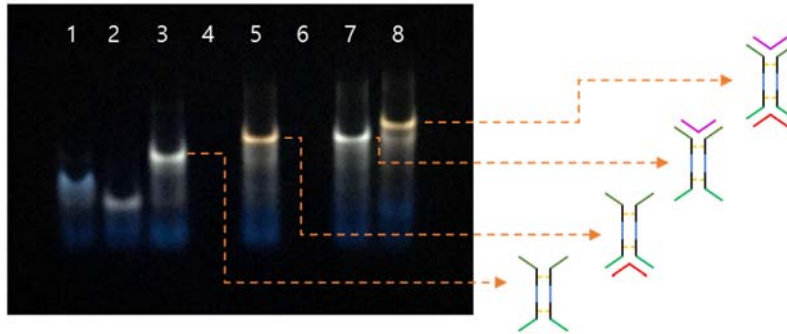


10% PAGE

(A) L 1 2 3 4 5 6 7 8 L



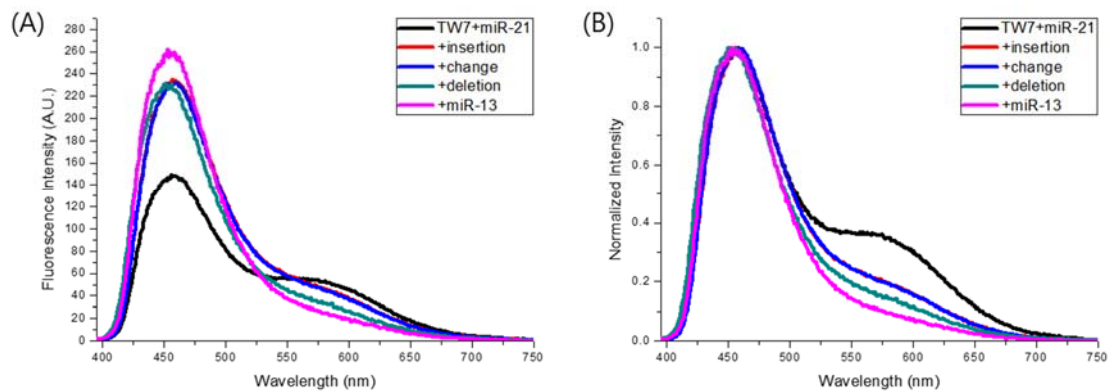
(B) 1 2 3 4 5 6 7 8



Lane	Sample
1	TW7-M1
2	TW7-M2
3	TW7-M1+TW7-M2
4	miR-21
5	TW7-M1+TW7-M2 +miR-21
6	miR-192
7	TW7-M1+TW7-M2 +miR-192
8	TW7-M1+TW7-M2 +miR-21+miR-192
L	DNA ladder (10 bp)

200 pmol ODNs in 50 mM Tris-HCl (pH 7.2) buffer, 100 mM NaCl, 10 mM MgCl₂

Figure S10. (A) Fluorescence emission spectra and (B) normalized fluorescence emission spectra of probes in the presence of RNAs.



miR-21 (22-mer): 5'- uag cuu auc **aga** cug aug uug a-3'
 Insertion (23-mer): 5'- uag cuu auc agga cug aug uug a-3'
 Change (22-mer): 5'- uag cuu auc aca cug aug uug a-3'
 Deletion (21-mer): 5'- uag cuu auc aa cug aug uug a-3'
 miR-13 (22-mer): 5'- uau cac agc cau uuu gau gag u-3'

Figure S11. Normalized fluorescence spectra of probes in the absence and presence of (A) miR-13, (B) miR-192, and (C) miR-221.

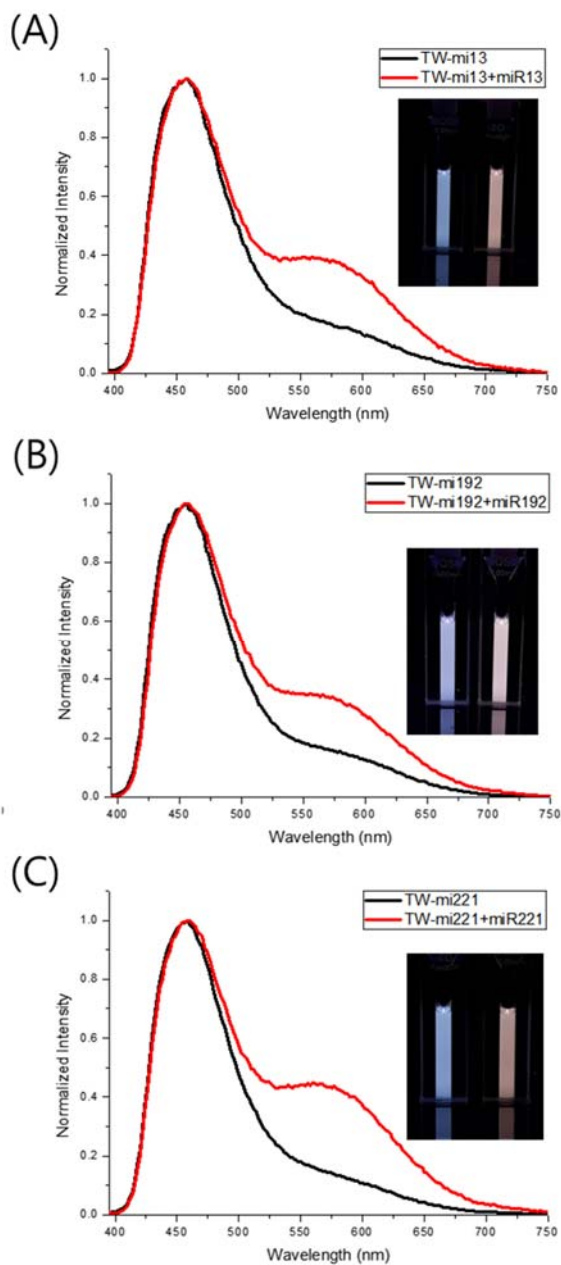


Figure S12. (A-C) Fluorescence emission spectra of **TW-m** series, and (D) The fluorescence intensity ratios compared at 455 and 600 nm, and (E) changes in the values of I_{455}/I_{600} in the presence or absence of miRNAs.

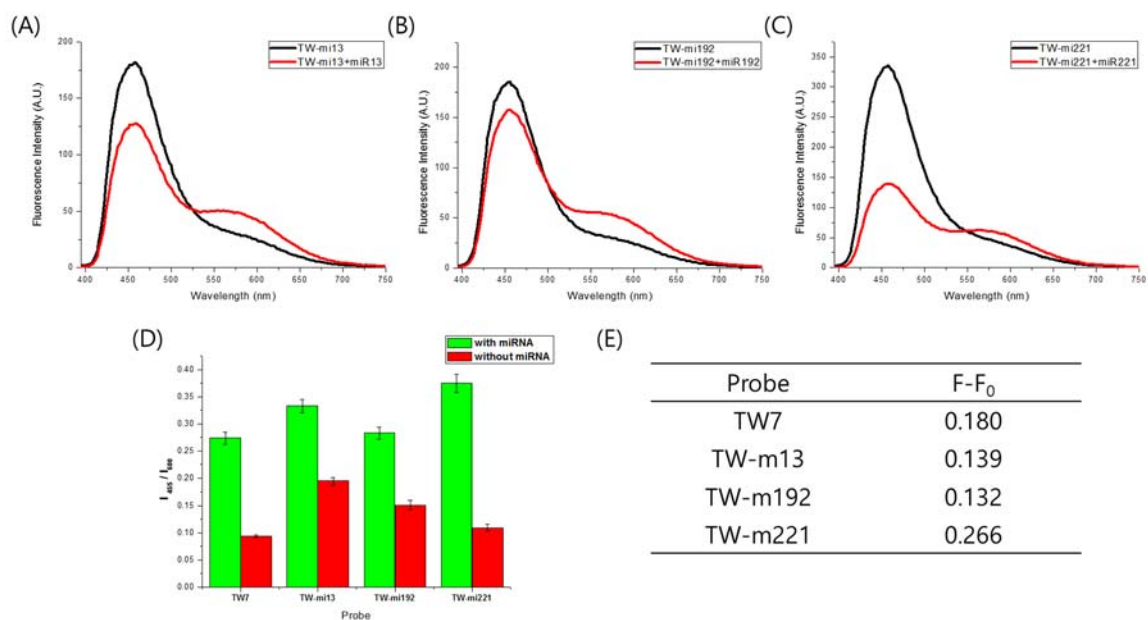


Table S4. Fluorescence emission peak areas of ^{Py}A -modified probes in the presence and absence of miRNAs.

ODNs	1 st area ^a	1 st area%	2 nd area ^b	2 nd area%	A_{long}/A_{short}
TW7+miR21	6148	43	8389	57	1.3645
TW-m13+miR-13	7467	46	8787	54	1.1768
TW-m192+miR-192	9144	51	8909	49	0.9743
TW-m221+miR-221	8336	47	9337	53	1.1200

ODNs	1 st area ^a	1 st area%	2 nd area ^b	2 nd area%	A_{long}/A_{short}
TW7	12285	59	8398	41	0.6836
TW-m13	10208	60	6802	40	0.6663
TW-m192	10567	61	6670	39	0.6312
TW-m221	18073	62	10915	38	0.6039

^a Area percentage of the fluorescence emission peak at 455 nm. ^b Area percentage of the fluorescence emission peak at 575 nm. All spectra were recorded for samples in buffer (50 mM Tris-HCl, 100 mM NaCl, 10 mM MgCl₂; pH 7.2) at 25 °C.

Figure S13. Confocal microscopy images of intracellular miR-21 in living HeLa cells, recorded in the presence of **TW7**. (A) Channel of pyrene monomer ($\lambda_{\text{ex}} = 405 \text{ nm}$; emission range: 455–495 nm); (B) channel of PyA -cluster ($\lambda_{\text{ex}} = 405 \text{ nm}$; emission range: 555–600 nm); (C) merged images from (A) and (B); (D) bright-field image; and (E) merged images with bright field image in (D). Scale bar: 10 μm .

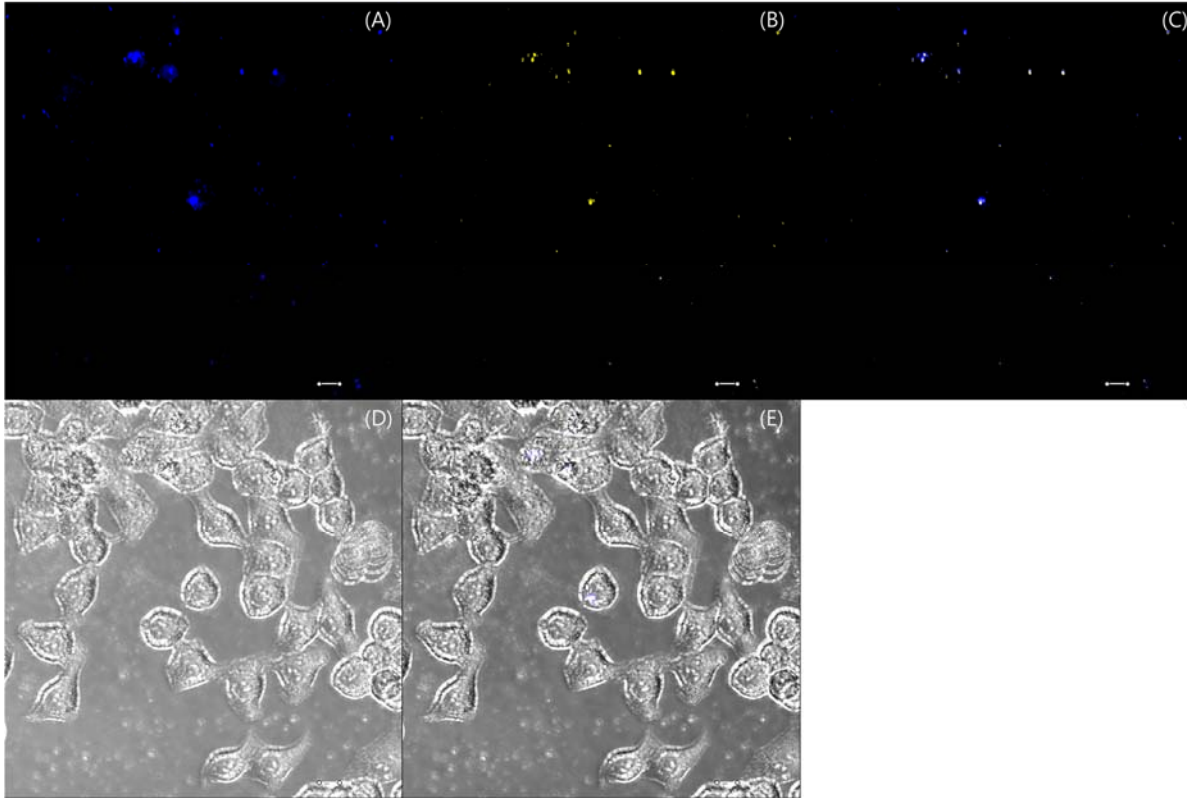
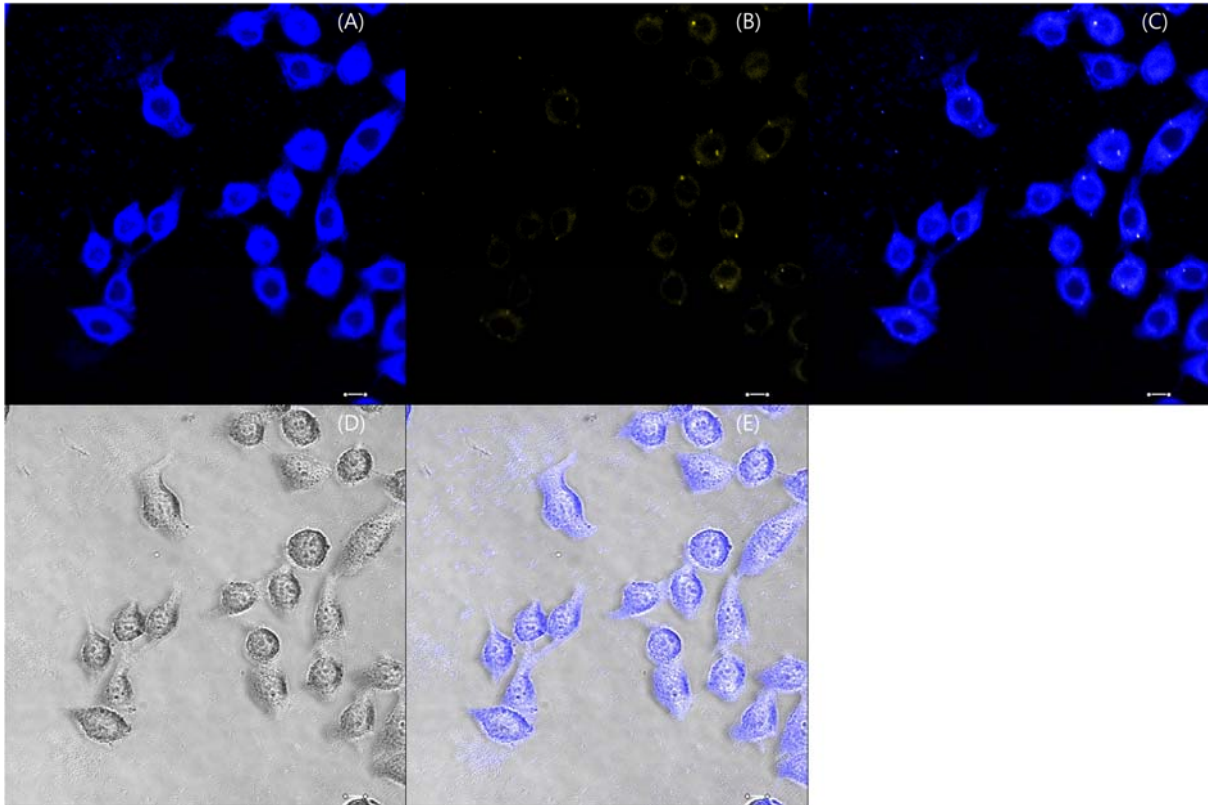


Figure S14. Confocal microscopy images of intracellular miR-21 in living HeLa cells, recorded in the absence of **TW7** (control). (A) Blue channel ($\lambda_{\text{ex}} = 405 \text{ nm}$; emission range: 455–495nm); (B) yellow channel ($\lambda_{\text{ex}} = 405 \text{ nm}$; emission range: 555–600 nm); (C) merged images from (A) and (B); (D) bright-field image; and (E) merged images with bright-field image in (D). Scale bar: 10 μm .



Figure S15. Confocal microscopic images of intracellular miR-21 target in living HeLa cells, recorded in the presence of **TW7-R**. (A) Blue channel ($\lambda_{\text{ex}} = 405 \text{ nm}$; emission range: 455–495 nm); (B) yellow channel ($\lambda_{\text{ex}} = 405 \text{ nm}$; emission range: 555–600 nm); (C) merged images from (A) and (B); (D) bright-field image; and (E) merged images with bright-field image in (D). Scale bar: 10 μm .



Name	Sequence
TW7-R	5'-ATC GAA TAG TC AA ^{Py} AAA CGCGCG AA ^{Py} AAA TCA ACA TCA GT-3'

Figure S16. Confocal microscopy images of intracellular miR-21 in living MCF-7 cells, recorded in the presence of **TW7**. (A) Channel of pyrene monomer ($\lambda_{\text{ex}} = 405 \text{ nm}$; emission range: 455–495 nm); (B) channel of ^{Py}A-cluster ($\lambda_{\text{ex}} = 405 \text{ nm}$; emission range: 555–600 nm); (C) merged images from (A) and (B); (D) bright-field image; and (E) merged images with bright field image in (D). Scale bar: 10 μm .

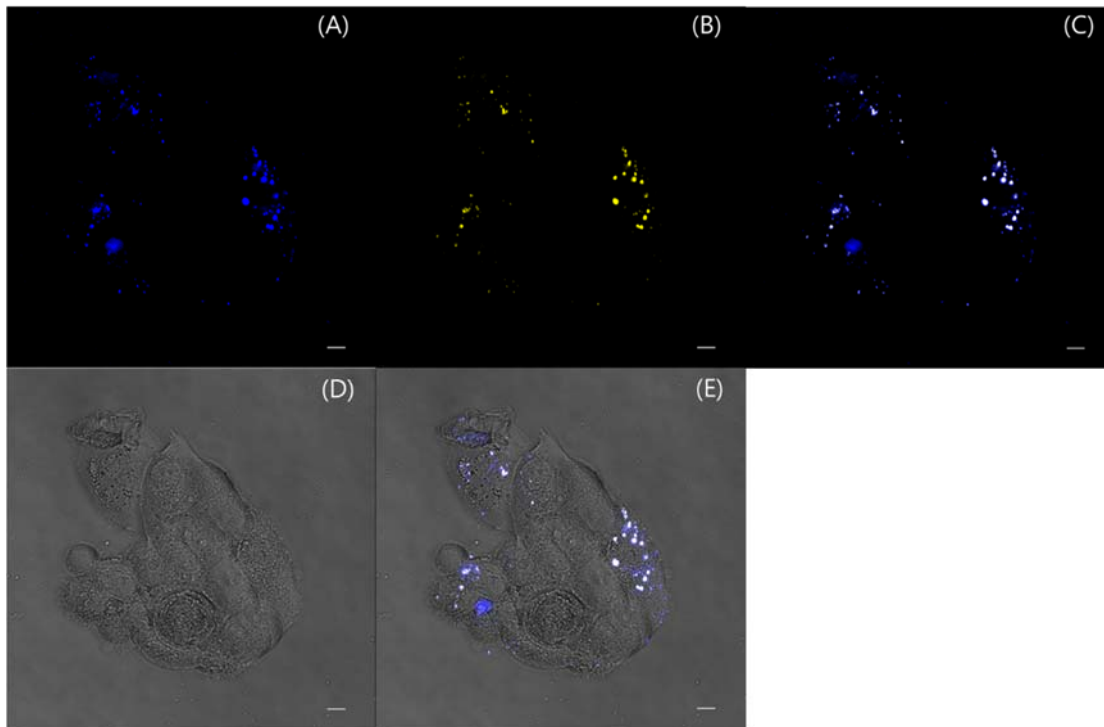


Figure S17. Confocal microscopy images of intracellular miR-21 in living MCF-7 cells, recorded in the absence of **TW7** (control). (A) Blue channel ($\lambda_{\text{ex}} = 405 \text{ nm}$; emission range: 455–495nm); (B) yellow channel ($\lambda_{\text{ex}} = 405 \text{ nm}$; emission range: 555–600 nm); (C) merged images from (A) and (B); (D) bright-field image; and (E) merged images with bright-field image in (D). Scale bar: 10 μm .

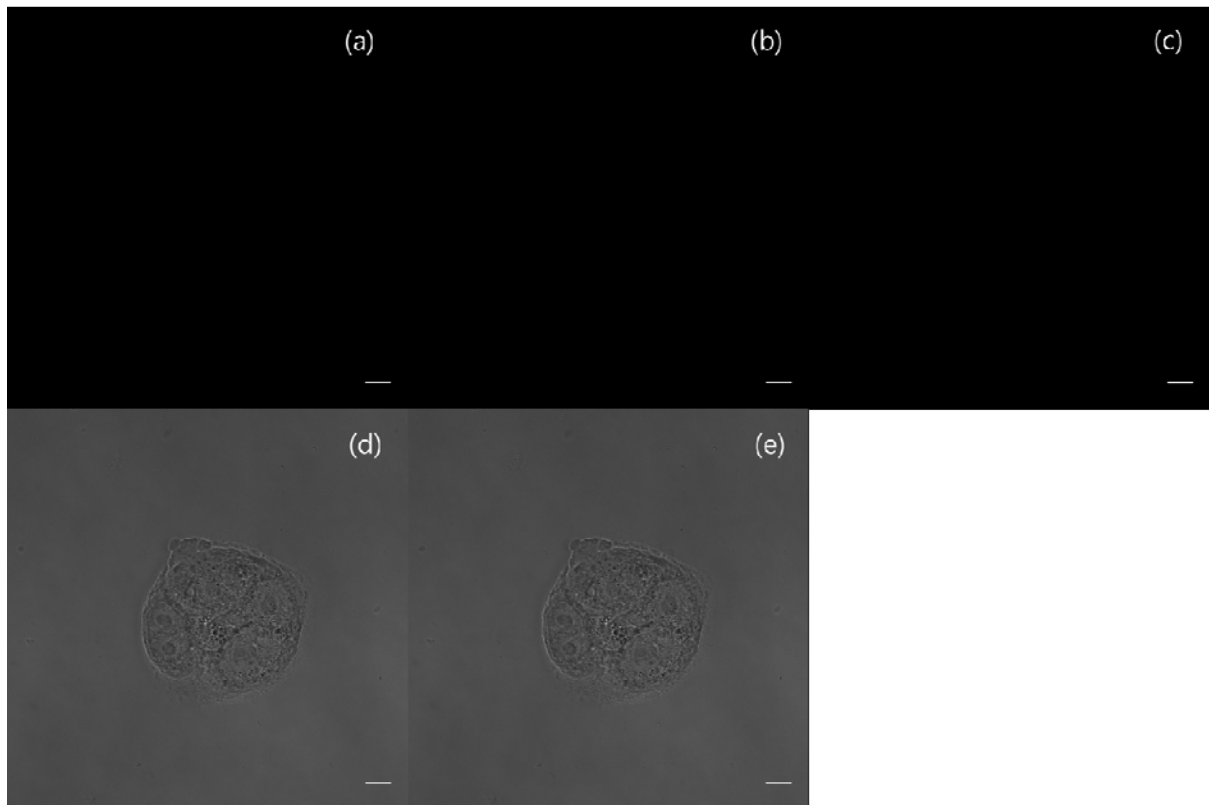
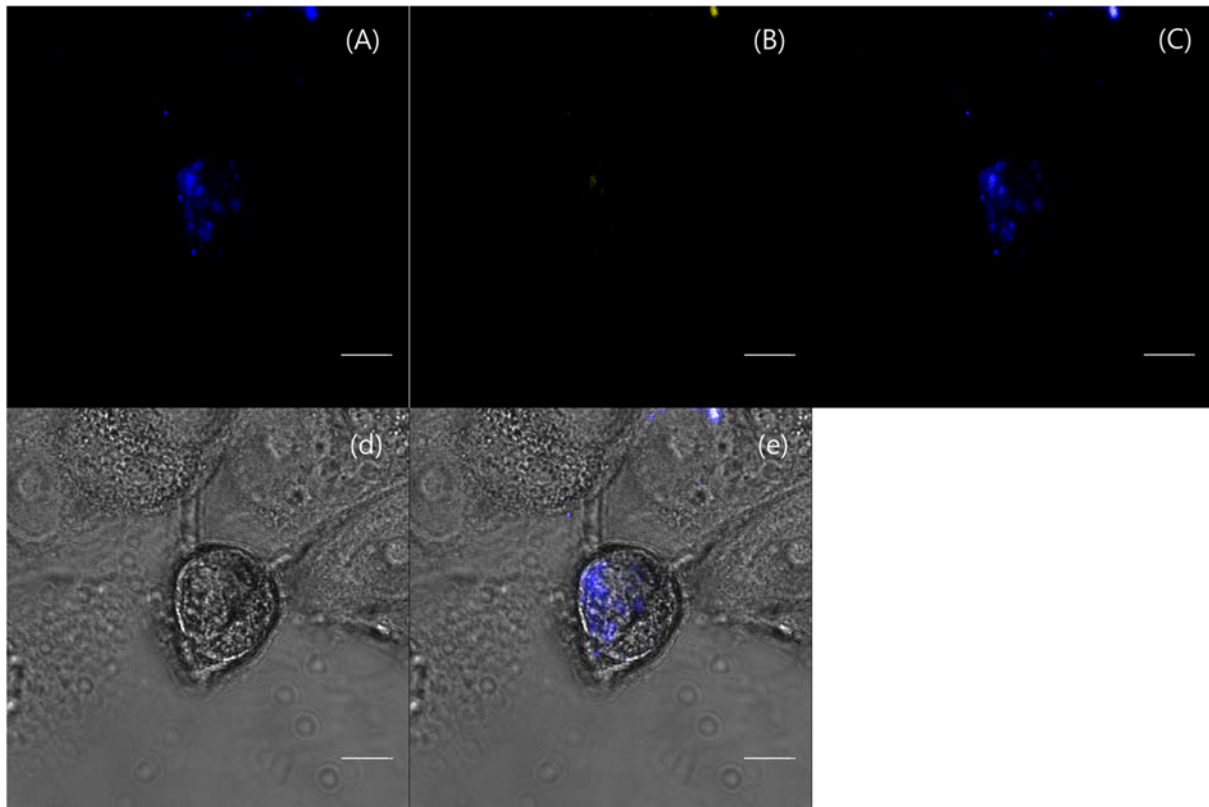


Figure S18. Confocal microscopic images of intracellular miR-21 target in living MCF-7 cells, recorded in the presence of **TW7-R**. (A) Blue channel ($\lambda_{\text{ex}} = 405 \text{ nm}$; emission range: 455–495 nm); (B) yellow channel ($\lambda_{\text{ex}} = 405 \text{ nm}$; emission range: 555–600 nm); (C) merged images from (A) and (B); (D) bright-field image; and (E) merged images with bright-field image in (D). Scale bar: 10 μm .



Name	Sequence
TW7-R	5'-ATC GAA TAG TC AA ^{Py} AAA CGCGCG AA ^{Py} AAA TCA ACA TCA GT-3'

Figure S19. Confocal microscopy images of intracellular miR-21 in living NIH-3T3 cells, recorded in the presence of **TW7**. (A) Channel of pyrene monomer ($\lambda_{\text{ex}} = 405 \text{ nm}$; emission range: 455–495 nm); (B) channel of ^{Py}A-cluster ($\lambda_{\text{ex}} = 405 \text{ nm}$; emission range: 555–600 nm); (C) merged images from (A) and (B); (D) bright-field image; and (E) merged images with bright field image in (D). Scale bar: 10 μm .

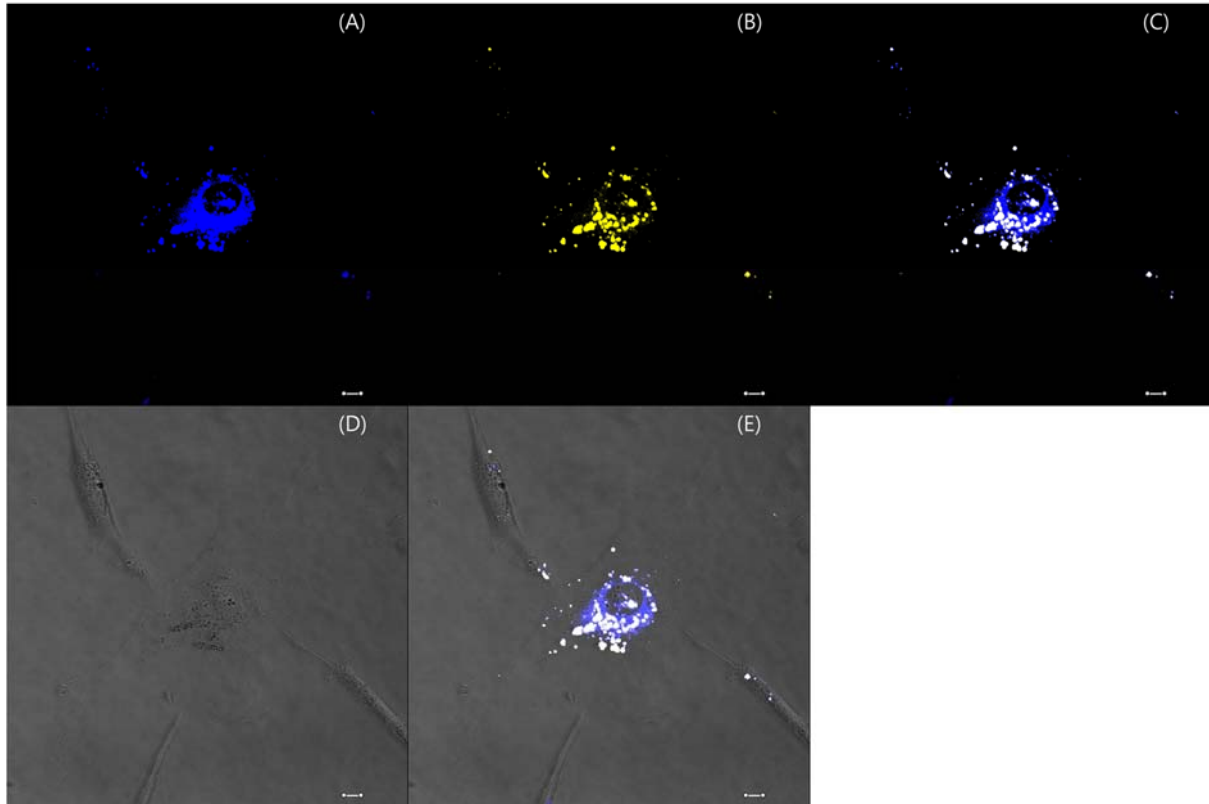


Figure S20. Confocal microscopy images of intracellular miR-21 in living NIH-3T3 cells, recorded in the absence of **TW7** (control). (A) Blue channel ($\lambda_{\text{ex}} = 405 \text{ nm}$; emission range: 455–495nm); (B) yellow channel ($\lambda_{\text{ex}} = 405 \text{ nm}$; emission range: 555–600 nm); (C) merged images from (A) and (B); (D) bright-field image; and (E) merged images with bright-field image in (D). Scale bar: 10 μm .

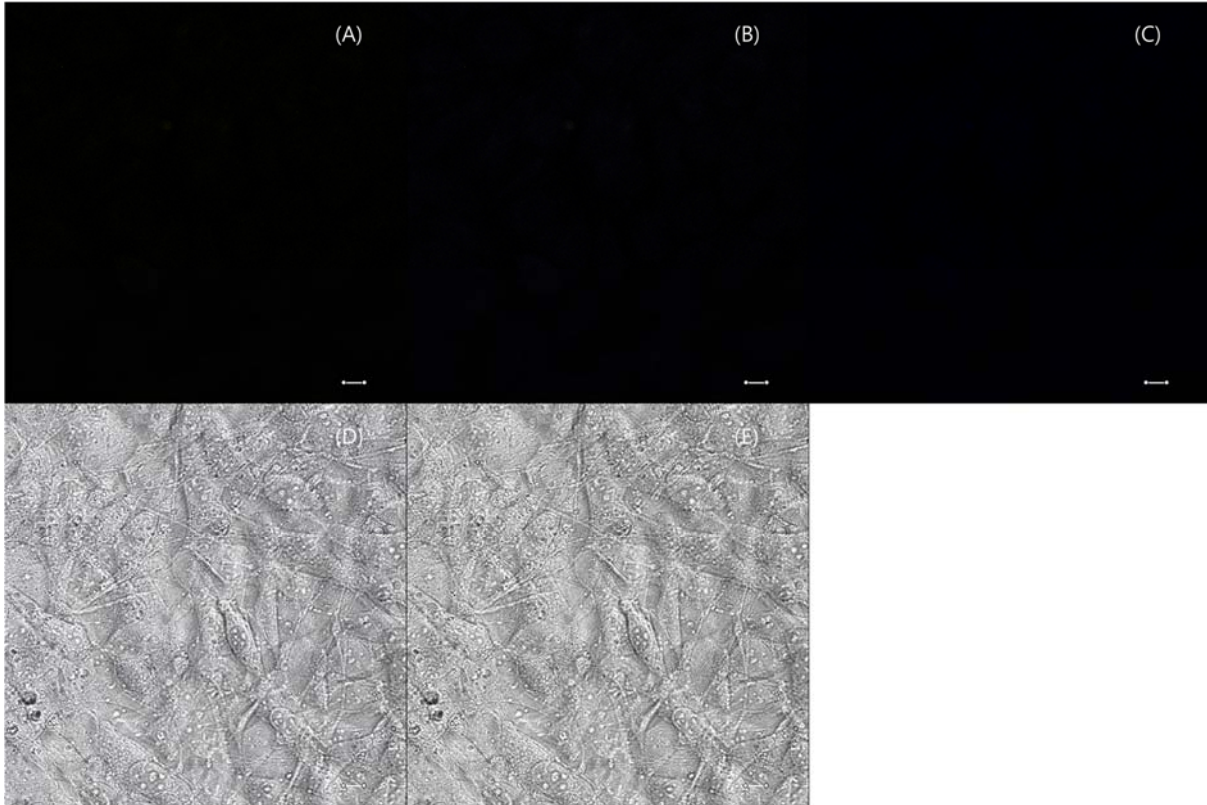
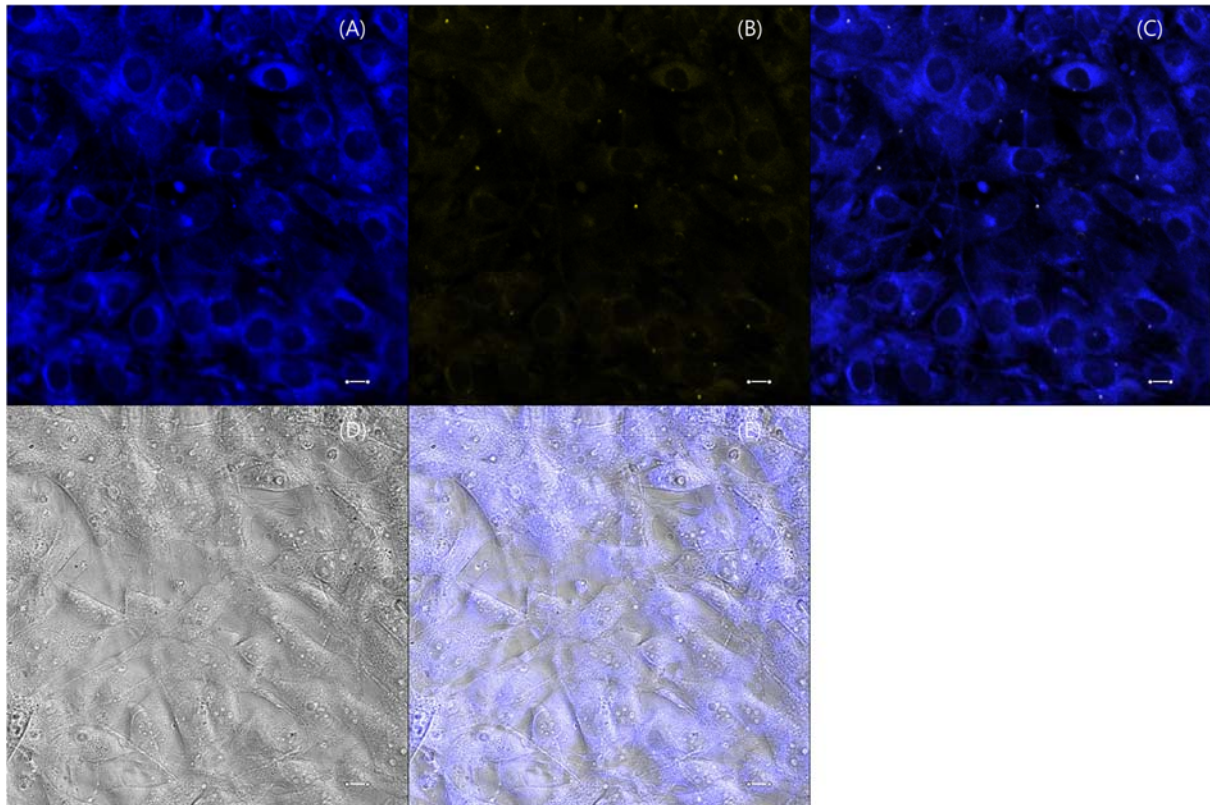


Figure S21. Confocal microscopic images of intracellular miR-21 target in living NIH-3T3 cells, recorded in the presence of **TW7-R**. (A) Blue channel ($\lambda_{\text{ex}} = 405 \text{ nm}$; emission range: 455–495 nm); (B) yellow channel ($\lambda_{\text{ex}} = 405 \text{ nm}$; emission range: 555–600 nm); (C) merged images from (A) and (B); (D) bright-field image; and (E) merged images with bright-field image in (D). Scale bar: 10 μm .



Name	Sequence
TW7-R	5'-ATC GAA TAG TC AA ^{Py} AAA CGCGCG AA ^{Py} AAA TCA ACA TCA GT-3'

Figure S22. z-Stack slice images of HeLa cells, from the surface to bottom, recorded under excitation at 405 nm (total depth: 31.62 μm).

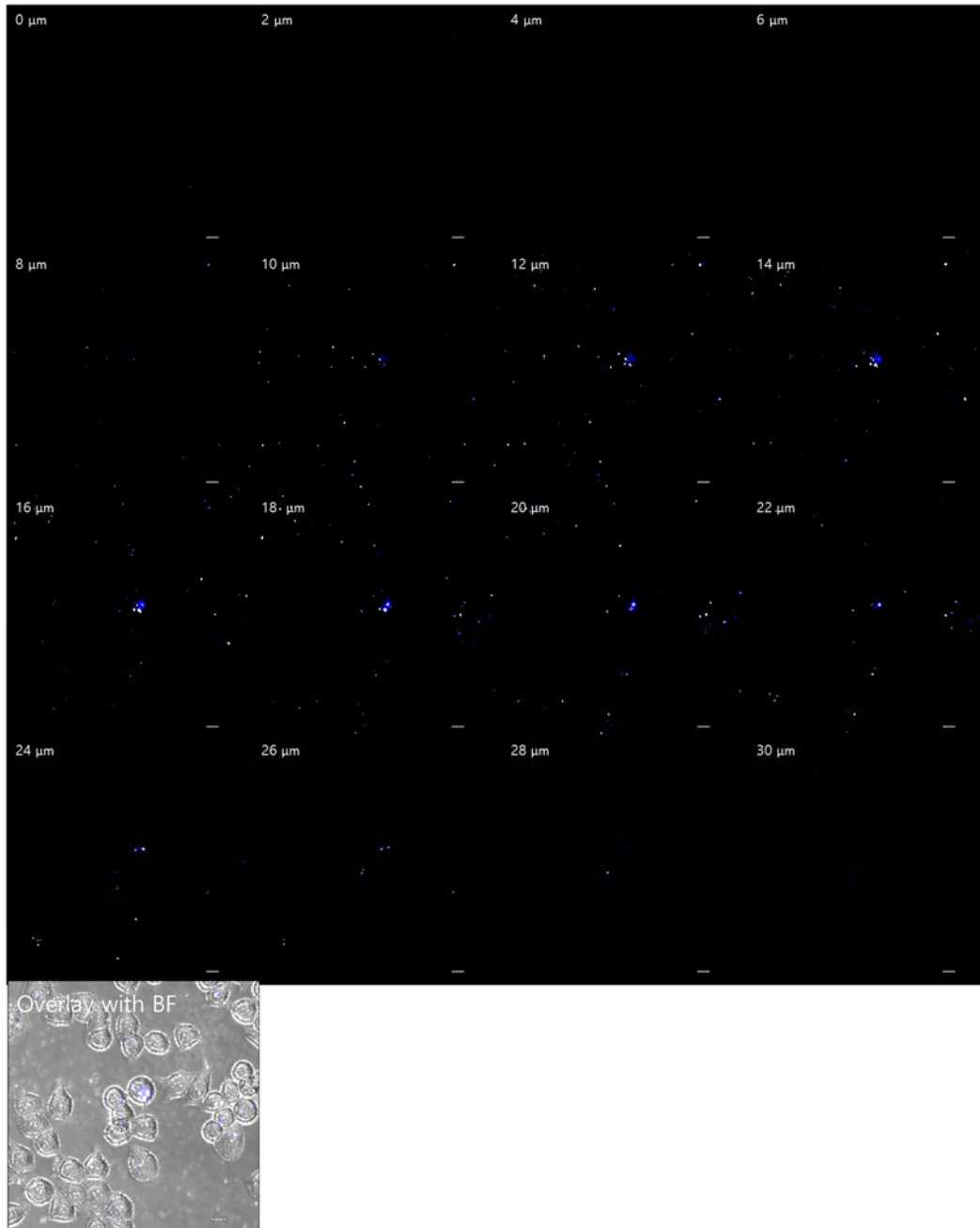


Figure S23. z-Stack slice images of MCF-7 cells, from the surface to bottom, recorded under excitation at 405 nm (total depth: 35.69 μm).

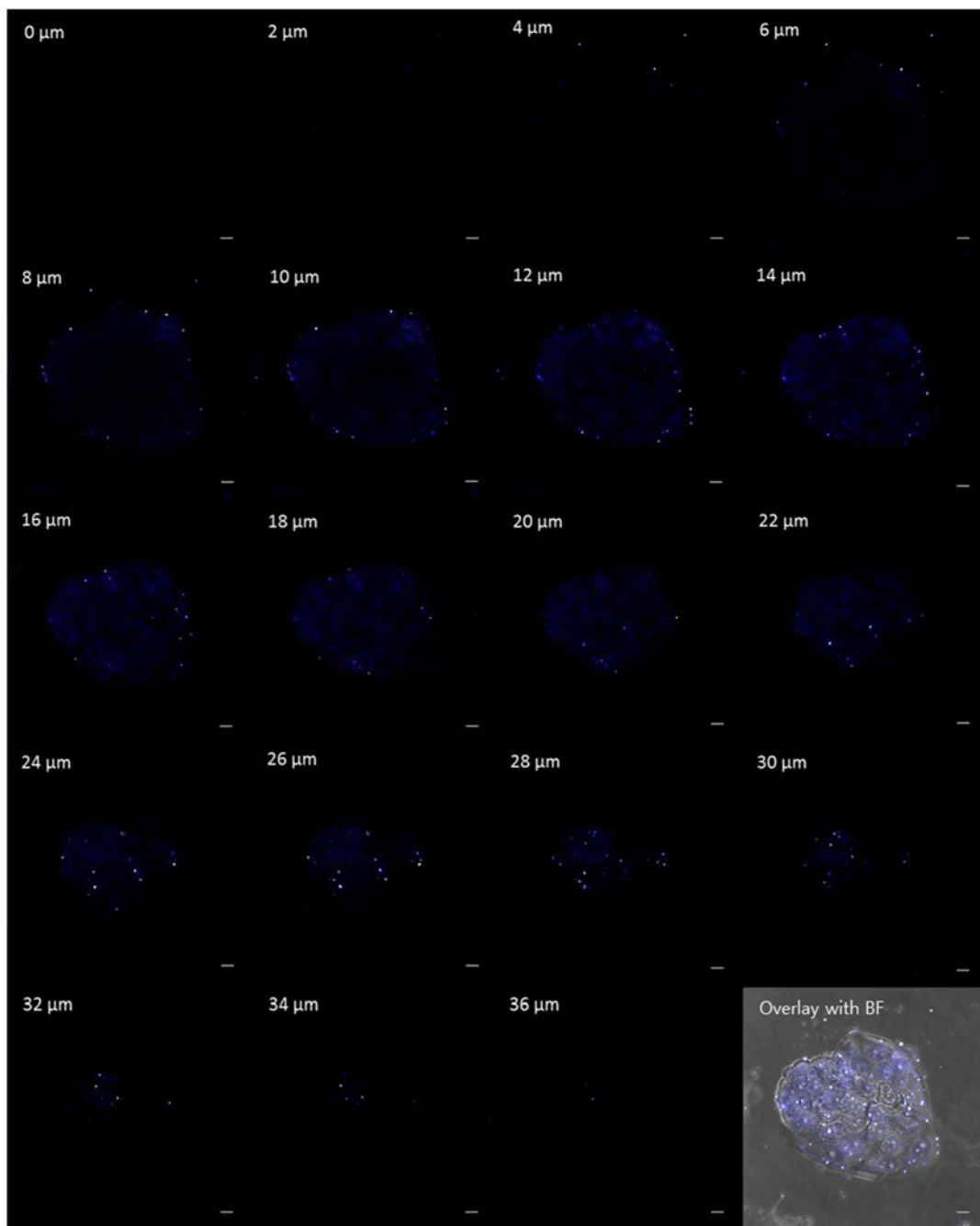
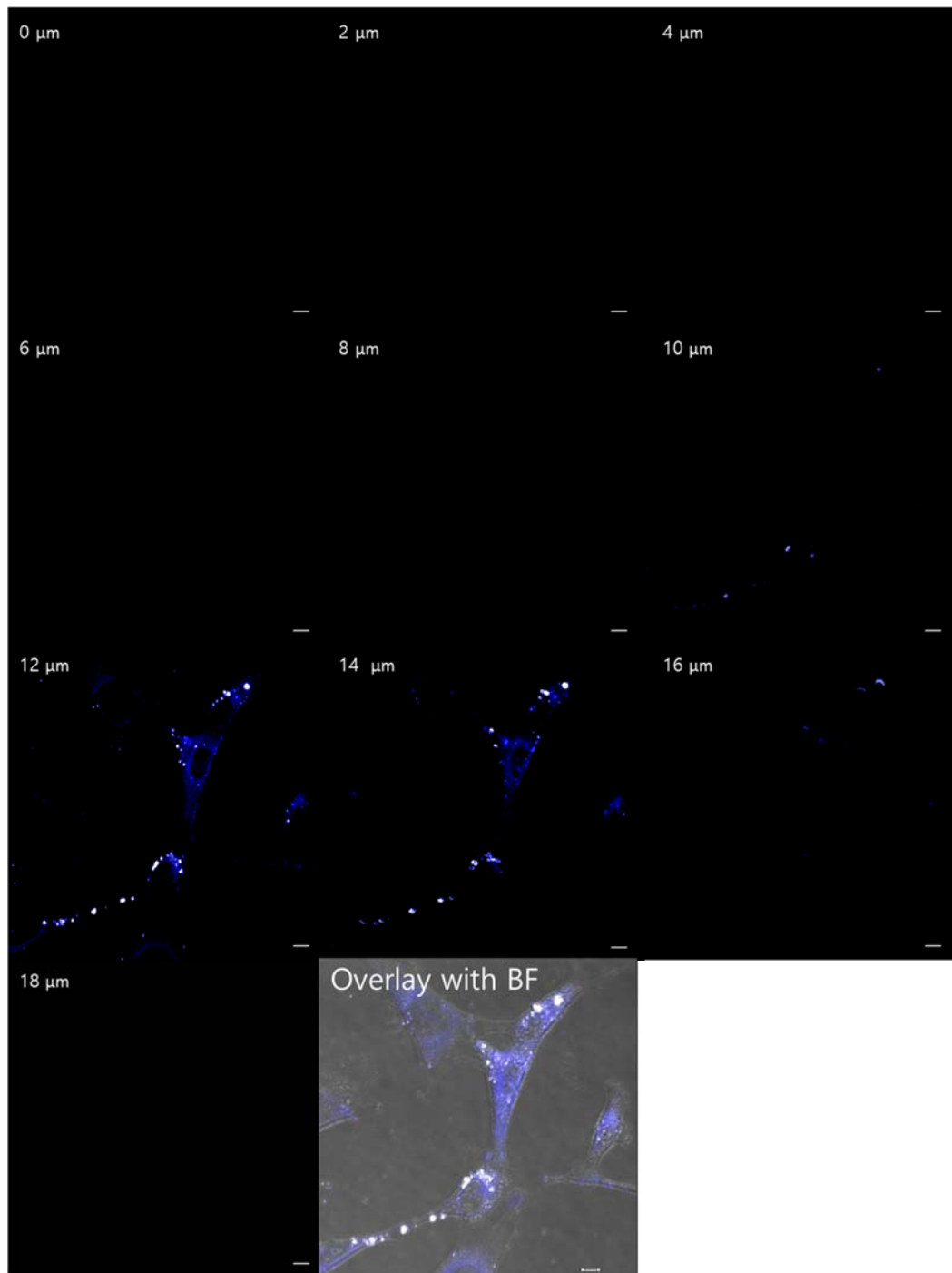


Figure S24. z-Stack slice images of NIH-3T3 cells, from the surface to bottom, recorded under excitation at 405 nm (total depth: 17.78 μm).



References

- 1 S. Pramanick, J. Kim, J. Kim, G. Saravanakumar, D. Park and W. J. Kim, *Bioconjugate Chem.*, 2018, **29**, 885–897.
- 2 H. Jo, H. Youn, S. Lee and C. Ban, *J. Mater. Chem. B*, 2014, **2**, 4862–4867.
- 3 Y. W. Jun, H. R. Kim, Y. J. Reo, M. Dai and K. H. Ahn, *Chem. Sci.*, 2017, **8**, 7696–7704.